Order parameter for the multichannel Kondo model at quantum criticality

Ru Zheng,* Rong-Qiang He,† and Zhong-Yi Lu‡
Department of Physics, Renmin University of China, Beijing 100872, China

(Received 2 September 2020; revised 24 December 2020; accepted 24 December 2020; published 11 January 2021)

A multichannel Kondo model, where two or more equivalent but independent channels of electrons compete to screen a spin-$\frac{1}{2}$ impurity, shows overcompensation of the impurity spin, leading to the non-Fermi-liquid behavior in various thermodynamic and transport properties. However, when the channel symmetry is broken, an impurity quantum phase transition can occur at zero temperature. Identification of an order parameter describing the impurity quantum phase transition is very difficult since it is beyond the conventional Landau-Ginzburg-Wilson theory. By employing the natural orbitals renormalization group method, we study both two-channel and three-channel Kondo models, from the perspective of spin correlation between the impurity and electrons in electronic channels. Here we demonstrate that by introducing the spin-correlation ratio as an order parameter we can characterize impurity quantum phase transitions driven by channel asymmetry. In particular, the universal critical exponents β of the spin-correlation ratio and ν of the correlation length are explicitly determined by finite-size-scaling analysis, namely, $\beta = 0.10(1)$ and $\nu = 2.0(1)$, and $\beta = 0.10(1)$ and $\nu = 2.5(1)$ for the two-channel and three-channel Kondo models, respectively.

DOI: 10.1103/PhysRevB.103.045111

I. INTRODUCTION

The Kondo effect [1,2], induced by the antiferromagnetic exchange interaction between a localized spin-$\frac{1}{2}$ impurity and conduction electrons in the Fermi sea, is an intensively studied problem in quantum many-body physics. Below a characteristic energy scale T_K, namely, the Kondo temperature, the magnetic impurity is collectively screened by the surrounding conduction electrons, leading to the Fermi-liquid behavior in low-temperature properties. The concise interpretation of the Kondo effect is through the well-known single-impurity Kondo model [1,3,4], whose ground state is a Kondo singlet. On the other hand, the Kondo screening is strongly modified if the magnetic impurity is coupled to two or more independent channels of electrons.

Nozières and Blandin [5] proposed a multichannel generalization of the standard Kondo model, i.e., the multichannel Kondo (MCK) model, where $M > 1$ equivalent but independent channels of electrons compete to screen a spin-$\frac{1}{2}$ impurity and then the impurity is ultimately overscreened. Correspondingly, the various physical properties have been studied by the Bethe ansatz [6–10], conformal field theory (CFT) [11–15], bosonization [16,17], and the numerical renormalization group (NRG) method[4,13,18], as well as other approaches [19,20]. At low temperatures, the spin-$\frac{1}{2}$ impurity is simultaneously screened by each channel, resulting in the non-Fermi-liquid behavior in various thermodynamic and transport properties. These nontrivial low-temperature properties include the nonvanishing zero-temperature impurity entropy $S_{\rm imp}(T=0) = \ln[2\cos(\frac{\pi}{2+M})]$ and the fractional power-law behavior of impurity magnetic susceptibility $\chi_{\rm imp} \propto T^{2\Delta-1}$ and of the impurity specific-heat ratio $\gamma_{\rm imp} = C_{\rm imp}/T \propto T^{2\Delta-1}$ for $T \to 0$, where $1+\Delta = 1+2/(2+M)$ is the scaling dimension of the leading irrelevant operator at the fixed point. In addition, the resistivity at low temperature goes as $R \propto T^{\Delta}$, which is different from that of the Fermi liquid with $R \propto T^2$. In particular, in the two-channel case $M = 2$, i.e., the two-channel Kondo (2CK) model, logarithmic corrections in the thermodynamic properties occur instead, leading to $\chi_{\rm imp} \propto \ln T$ and $\gamma_{\rm imp} \propto \ln T$ for $T \to 0$ with an anomalous Wilson ratio $R_W = \chi_{\rm imp}/\gamma_{\rm imp} = \frac{8}{3}$, in contrast to the result of the standard single-impurity Kondo model $R_W = \frac{8}{4} = 2$. On the experimental side, several realizations of the 2CK effect have also been obtained [21–27].

The above anomalous low-temperature properties of an MCK system are based on the condition that all the channels are equivalent, namely, symmetric. However, the non-Fermi-liquid physics is extremely delicate against the channel symmetry-breaking perturbation: Even the smallest asymmetry destabilizes the non-Fermi-liquid fixed point in the renormalization group (RG) flow. For instance, in the 2CK model with J_a and J_b denoting the two Kondo couplings, when the channel symmetry is broken ($J_a \neq J_b$), a new temperature scale $T^* \propto (J_a - J_b)^2$, along with a corresponding length scale $\xi^* \sim 1/T^*$, for the crossover from the unstable overscreened non-Fermi-liquid fixed point to the stable fully screened Fermi-liquid fixed point has been found [18,28]. In this case, T^* characterizes the energy scale for flow away from the overscreened fixed point at intermediate temperatures and the impurity is hence completely screened by the channel with the stronger coupling at $T = 0$. Only on fine-tuning the Kondo couplings $J_a \to J_b$ to the symmetry point with $T^* \to 0$, one obtains the non-Fermi-liquid physics at the

*zhengru@ruc.edu.cn
†rqhe@ruc.edu.cn
‡zlu@ruc.edu.cn

lowest-energy scales. Therefore, at $T = 0$, an MCK system may undergo an impurity quantum phase transition (IQPT) [29] driven by channel asymmetry, where only the impurity contribution to the free energy becomes singular at the critical point. The simple physical picture is that one channel couples to the impurity more strongly than the rest and then the impurity is screened only by this channel while the other channels decouple, leading to the standard 1CK physics with a Fermi-liquid phase [5,20,30]. An IQPT can then occur at the channel-symmetric point as the channel asymmetry is varied.

To describe a phase transition, we need to introduce an order parameter. However, interpretation for IQPTs goes beyond the classical Landau-Ginzburg-Wilson scenario due to the fact that an IQPT is distinct from any bulk phase transitions, and thus identification of an order parameter describing an IQPT is very difficult. Recently, much effort has been made to explore order parameters characterizing an IQPT [31–33]. Inspired by quantum information, the Schmidt gap [31] and negativity [32] have been introduced as order parameters to describe the IQPT in a 2CK model. Nevertheless, there is a still lack of order parameters based on correlation functions, especially an observable one.

In this work, using the natural orbitals renormalization group (NORG) method [34], we explore such order parameters to describe the IQPTs driven by the channel asymmetry in both 2CK and 3CK models, from the perspective of spin correlation between the impurity and electrons in the electronic channels. The corresponding universal critical exponents can be further extracted by finite-size-scaling analysis.

This paper is organized as follows. In Sec. II the 2CK and 3CK models and the NORG numerical method are introduced. In Sec. III we study the spin correlation between the impurity and electrons in electronic channels. The spin-correlation ratio is then introduced and further demonstrated as an appropriate order parameter to describe the IQPTs driven by the channel asymmetry in both models. Finally, by finite-size-scaling analysis, we explicitly determine the universal critical exponents β of the spin-correlation ratio and ν of the correlation length to be $\beta = 0.10(1)$ and $\nu = 2.0(1)$, and $\beta = 0.10(1)$ and $\nu = 2.5(1)$ for the 2CK and 3CK models, respectively. Section IV gives a short discussion and Sec. V summarizes this work.

II. MODELS AND NUMERICAL METHOD

Generally, the Hamiltonian for an MCK model, where M independent channels of electrons compete to screen a single spin-$\frac{1}{2}$ impurity, can be written as $H_{\rm MCK} = \sum_a H_a + H_{\rm int}$, with

$$H_a = \sum_{k\sigma} \varepsilon_k c^\dagger_{ak\sigma} c_{ak\sigma},$$
$$H_{\rm int} = \sum_a J_a \mathbf{S}_0 \cdot \mathbf{s}_{a1}, \tag{1}$$

where $a = 1, 2, \ldots, M$ is the electronic channel index. The operator $c^\dagger_{ak\sigma}$ creates an electron at a Bloch state with a wave vector k and spin $\sigma = \uparrow, \downarrow$ in channel a with ε_k denoting the dispersion relation. The impurity spin $\mathbf{S}_0$ is coupled to the electron spin $\mathbf{s}_{a1}$ at site 1 in channel a via Kondo coupling J_a. Here we consider the tight-binding chain emulation of the MCK model, as shown in Fig. 1, in which a localized spin-$\frac{1}{2}$ impurity is coupled to M independent periodic tight-binding chains by an antiferromagnetic exchange interaction.

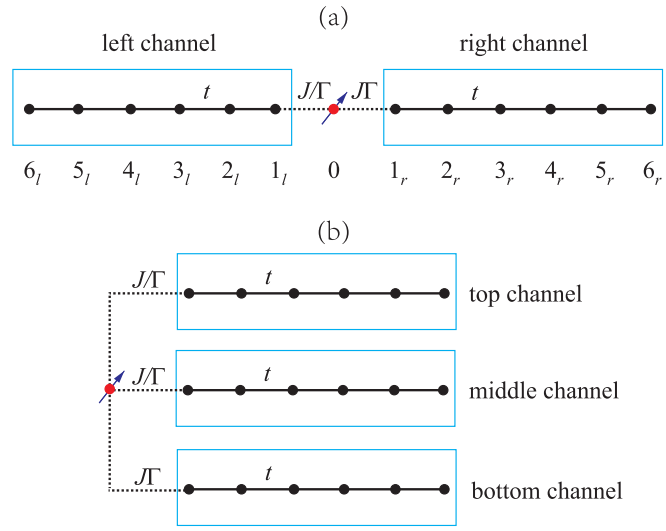

FIG. 1. Schematics of the (a) 2CK and (b) 3CK models with the electronic channels being simulated by independent periodic tight-binding chains. (a) A spin-$\frac{1}{2}$ impurity is coupled to its left and right channels by Kondo couplings $J_l = J/\Gamma$ and $J_r = J\Gamma$, respectively, with Γ standing for the asymmetry parameter. For $\Gamma = 1$, the impurity is overscreened by both channels, resulting in the 2CK physics, while for $\Gamma \neq 1$ in the thermodynamic limit, the impurity is screened only by the channel with the stronger coupling, representing the 1CK physics. (b) A spin-$\frac{1}{2}$ impurity is coupled to the top, middle, and bottom electronic channels with Kondo couplings $J_t = J_m = J/\Gamma$ and $J_b = J\Gamma$. The 3CK physics occurs at the symmetric point $\Gamma = 1$ while the impurity is screened simultaneously by all the channels. For any $\Gamma < 1$, the 2CK physics emerges with the impurity being overscreened by the top and middle channels, while the bottom channel decouples. In contrast, for any $\Gamma > 1$, the 1CK physics emerges with the impurity being screened only by the bottom channel.

A typical model for studying IQPTs in the MCK system is the 2CK model, where there exists a nontrivial critical crossover at the channel-symmetric point with the impurity being overscreened by the two channels. As illustrated in Fig. 1(a), the Hamiltonian for the 2CK model is given by $H_{\rm 2CK} = \sum_a H_a + H_{\rm int}$, with

$$H_a = -t \sum_{ij\sigma} (c^\dagger_{ai\sigma} c_{aj\sigma} + \text{H.c.}),$$
$$H_{\rm int} = \frac{J}{\Gamma} \mathbf{S}_0 \cdot \mathbf{s}_{l1} + J\Gamma \mathbf{S}_0 \cdot \mathbf{s}_{r1}. \tag{2}$$

Here $c^\dagger_{ai\sigma}$ ($c_{ai\sigma}$) represents the creation (annihilation) operator of a conduction electron at site i in channel $a \in \{l, r\}$ and $\mathbf{s}_{a1} = \frac{1}{2} \sum_{\alpha\beta} c^\dagger_{a1\alpha} \sigma_{\alpha\beta} c_{a1\beta}$, with σ representing the vector of Pauli matrices. The system size is $N = L + 1 = N_l + N_r + 1$, with N_a denoting the number of sites in channel a and L the number of total sites in all the electronic channels, and we take $N_l = N_r$ in this work. We keep the Kondo couplings $J_l = J/\Gamma$ and $J_r = J\Gamma$, where the dimensionless quantity Γ plays a controlling role. The system presents critical behavior around

$\Gamma = 1$, where the two channels are symmetric with $J_l = J_r$, resulting in the 2CK physics with a non-Fermi-liquid phase. For any $\Gamma \neq 1$ in the thermodynamic limit $N \to \infty$, the 1CK physics with a Fermi-liquid phase emerges and the impurity is screened only by the channel with the stronger coupling, while the other channel decouples. Hence, the $\Gamma = 1$ point acts as a critical point separating the two phases.

Another typical model we consider is the 3CK model. Likewise, the Hamiltonian for the 3CK model presented in Fig. 1(b) can be given by $H_{3\mathrm{CK}} = \sum_a H_a + H_{\mathrm{int}}$, with

$$H_{\mathrm{int}} = \frac{J}{\Gamma}\mathbf{S}_0 \cdot \mathbf{s}_{t1} + \frac{J}{\Gamma}\mathbf{S}_0 \cdot \mathbf{s}_{m1} + J\Gamma\mathbf{S}_0 \cdot \mathbf{s}_{b1}. \tag{3}$$

Here a spin-$\frac{1}{2}$ impurity is coupled to three [top (t), middle (m), and bottom(b)] tight-binding chains with Kondo couplings $J_t = J_m = J/\Gamma$ and $J_b = J\Gamma$. Again, the system size is $N = L + 1 = \sum_a N_a + 1$, with $a \in \{t, m, b\}$ and L denoting the number of total sites in all the electronic channels, and we take $N_t = N_m = N_b$ in this work. The 3CK physics with a non-Fermi-liquid phase occurs around the critical point $\Gamma = 1$, where the Kondo couplings to all the channels are equal, namely, the three channels are symmetric, and thus the impurity is overscreened by all the channels. For any $\Gamma > 1$ in the thermodynamic limit $N \to \infty$, the impurity is screened only by the bottom channel, leading to the emergence of the standard 1CK physics. In contrast, for any $\Gamma < 1$, the 2CK physics emerges with the top and middle channels equally competing for screening the impurity, while the bottom channel decouples. As a result, the channel-symmetric 3CK point $\Gamma = 1$ separates two distinct phases, namely, the 2CK non-Fermi-liquid phase for $\Gamma < 1$ and the 1CK Fermi-liquid phase for $\Gamma > 1$. Recently, the global phase diagram of the three-channel spin-orbital Kondo model, which is relevant for Hund metals, was studied using the NRG method [35].

We adopted the NORG approach to study the critical behavior in the 2CK and 3CK models. The NORG method works efficiently on quantum impurity models in the whole coupling regime and it preserves the whole geometric information of a lattice [34,36,37]. We emphasize that the effectiveness of the NORG is independent of any topological structure of a lattice. The NORG method works in the Hilbert space constructed from a set of natural orbitals [34,38]. Its realization essentially involves a representation transformation from a site representation into a natural orbital representation through iterative orbital rotations. In practice, to efficiently realize the NORG approach, we rotate only the orbitals of the bath, that is, only the bath orbitals are transformed into a natural orbital representation. By using the NORG method we can solve hundreds of noninteracting bath sites with any topological structures, while the computational cost is about $O(N_{\mathrm{bath}}^3)$, with N_{bath} the number of bath sites.

Throughout the work, we take an even number of sites in each channel, in which case the particle-hole symmetry is preserved. We set the nearest-neighbor hopping integral $t = \frac{1}{2}$ and keep half-filling of the conduction bands. All the calculations are carried out in the subspace of $S^z_{\mathrm{total}} = \frac{1}{2}$.

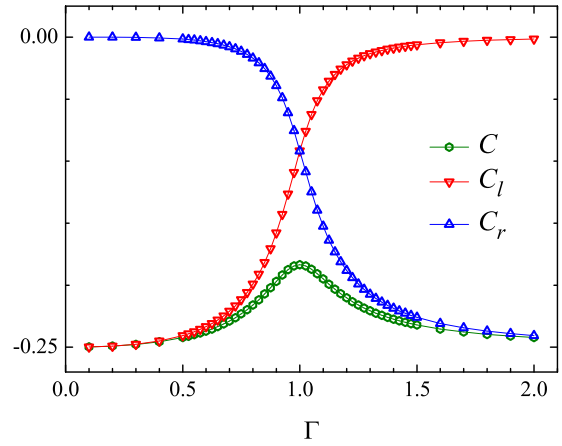

FIG. 2. Ground-state spin correlations C, C_l, and C_r between the localized impurity and electrons in the electronic channels in the 2CK model, versus Γ for a system of size $N = 205$ with the fixed coupling $J = 1$.

III. SPIN-CORRELATION RATIO AS AN ORDER PARAMETER

Screening of the single magnetic impurity in an MCK model by the electronic channels, whether full screening as in the standard 1CK physics or overscreening as in the 2CK and 3CK physics, certainly manifests itself in the structure of the spin correlation between the localized impurity and electrons in the electronic channels in the ground state. Moreover, the spin correlation may be measured by spin-polarized scanning tunneling microscopy. To be specific, the spin correlation between the impurity and electrons at site i in channel a has the form

$$C_a(i) = \langle 0|S_0^z s_{ai}^z|0\rangle, \tag{4}$$

where $|0\rangle$ denotes the ground state. We then consider the total correlation in channel a as well as in all the channels, which are given by

$$C_a = \sum_i C_a(i) = \sum_i \langle 0|S_0^z s_{ai}^z|0\rangle,$$
$$C = \sum_a C_a = \sum_{ai} \langle 0|S_0^z s_{ai}^z|0\rangle. \tag{5}$$

We first take the 2CK model (2) illustrated in Fig. 1(a) into consideration. When the two channels are symmetric, namely, $J_l = J_r$, the 2CK physics is valid with the impurity being overscreened by the two channels, where the temperature scale $T^* \propto (J_l - J_r)^2$ vanishes and the diverging length scale ξ^* ($\sim 1/T^*$) $\to \infty$ emerges in the thermodynamic limit. On the other hand, in the channel-asymmetric case, the standard 1CK physics emerges, where the magnetic impurity is screened only by the channel with the stronger coupling in the thermodynamic limit, while the other channel decouples. It is thus expected that the total correlation in a decoupled channel is 0, namely, $C_a = 0$, with a representing the decoupled channel, meaning that there is no correlation between this channel and the impurity.

We have studied the 2CK model by using the NORG method. In Fig. 2 we plot the calculated total correlations C,

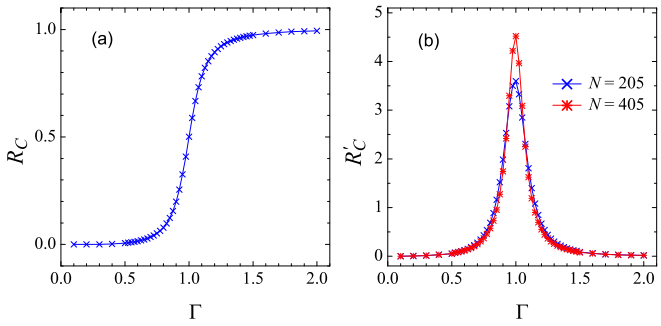

FIG. 3. (a) Spin-correlation ratio R_C as a function of Γ for a system of size $N = 205$ and (b) derivative of R_C with respect to Γ, namely, $R'_C = \partial R_C/\partial\Gamma$, for systems of sizes $N = 205$ and $N = 405$ with fixed coupling $J = 1$ in the 2CK model.

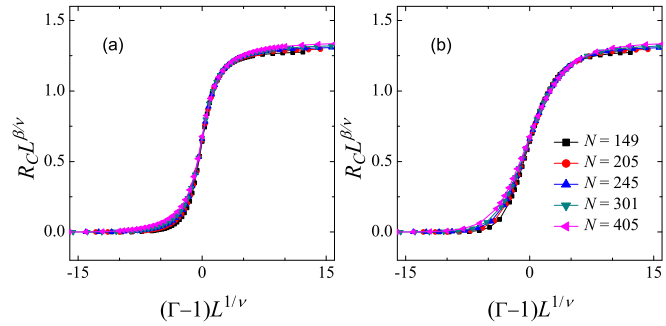

FIG. 4. Finite-size scaling of the spin-correlation ratio R_C with Kondo couplings (a) $J = 1.0$ and (b) $J = 0.5$ in the 2CK model. The obtained values are $\beta = 0.10 \pm 0.01$ and $\nu = 2.0 \pm 0.1$.

C_l, and C_r as functions of Γ with the fixed coupling $J = 1$. As the figure shows, when the parameter $\Gamma \ll 1$, $C_r \to 0$ and $C_l \to -\frac{1}{4}$, indicating that the impurity is correlated only with the left channel. In contrast, the impurity is correlated only with the right channel for $\Gamma \gg 1$. The correlations C_l and C_r cross at the critical point $\Gamma = 1$, where the 2CK physics is valid with the impurity being equally correlated with the two channels. It is expected that for any $\Gamma \neq 1$ in the thermodynamic limit, the correlation in channel a with smaller coupling $C_a \to 0$ while $C_{\bar{a}} \to -\frac{1}{4}$, where $\bar{a}$ denotes the other channel with the stronger coupling. Deviations of C_a and C from the values in thermodynamic limit in Fig. 2 result from the finite-size effect of the system we choose.

We hence introduce the spin-correlation ratio R_C in the form

$$R_C = \frac{C_r}{C} = \frac{\sum_i \langle 0|S_0^z s_{ri}^z|0\rangle}{\sum_{ai}\langle 0|S_0^z s_{ai}^z|0\rangle}. \tag{6}$$

At the channel-symmetric point $\Gamma = 1$, the overscreened impurity is correlated equally with the two channels, leading to $R_C = \frac{1}{2}$, while for any $\Gamma \neq 1$, the impurity is correlated only with the channel with the stronger coupling, while the other channel decouples. As a result, the value of R_C is expected to go from 0 to 1 around the critical point $\Gamma = 1$. Indeed, such a behavior of R_C is confirmed by the NORG calculations, as shown in Fig. 3(a). The thermodynamic limit behavior can be examined by further studying the derivative of the correlation ratio with respect to Γ, i.e., $R'_C = \partial R_C/\partial\Gamma$, which is plotted in Fig. 3(b). Figure 3(b) clearly shows that the derivative peaks at the critical point $\Gamma = 1$ and this peak becomes more pronounced as the system size N increases. This indicates that R'_C tends to diverge at the critical point $\Gamma = 1$ as $N \to \infty$, illustrating that the Kondo singlet in 1CK physics is destroyed and the overscreened ground state in 2CK physics emerges when Γ tends to 1 from $\Gamma \neq 1$. Therefore, we adopt the spin-correlation ratio R_C as an order parameter to characterize the IQPT in the 2CK model driven by the channel asymmetry.

In practical calculations, to characterize the critical behavior around a critical point, we need to do finite-size-scaling analysis [39–42] for an order parameter [43]. It has been known that a diverging characteristic length ξ emerges at the critical point g_c for a quantum phase transition, which scales as $\xi^{-1} \sim |g - g_c|^\nu$, with ν a critical exponent and g a control parameter. Meanwhile, an order parameter scales as $|g - g_c|^\beta$ in the vicinity of the critical point, where β is a critical exponent. It is emphasized that ν is uniquely determined by the system Hamiltonian. Here in the 2CK model, the correlation length is taken as the critical crossover scale ξ^* at which the RG flow crosses over from the overscreened 2CK fixed point to the fully screened Fermi-liquid fixed point.

For the spin-correlation ratio R_C in the 2CK model, we adopt a standard finite-size-scaling form

$$R_C(L) = L^{-\beta/\nu} F((\Gamma - 1)L^{1/\nu}), \tag{7}$$

where F is a scaling function and L the number of total sites in all the electronic channels. The order parameter R_C should show a scale-invariant behavior around the critical point $\Gamma = 1$, and thus we plot $R_C L^{\beta/\nu}$ as a function of $(\Gamma - 1)L^{1/\nu}$ in Figs. 4(a) and 4(b) for Kondo couplings $J = 1.0$ and $J = 0.5$, respectively. We explore the values of β and ν such that the curves for different system sizes N collapse on each other. When $\nu = 2.0 \pm 0.1$ and $\beta = 0.10 \pm 0.01$, all the curves in Figs. 4(a) and 4(b) respectively collapse to a single one, indicating that a very good data collapse is achieved. The value of the critical exponent $\nu = 2$ is in agreement with the result of CFT and bosonization [12,20,44], as well as with the analysis based on the Schmidt gap and negativity [31–33]. This demonstrates that R_C is an appropriate order parameter for characterizing the IQPT in the 2CK model.

We proceed with considering the 3CK model. At the channel-symmetric point, the 3CK physics is valid with the impurity being overscreened by all the channels, whereas when one of the Kondo couplings J_a is increased (or decreased), the 3CK fixed point crosses over to a Fermi-liquid fixed point with the impurity being screened only by this channel (or to a 2CK fixed point with the impurity being overscreened by the other two channels) on the new temperature scale of $T^* \propto |J_a - J_a^c|^{2.5}$, with J_a^c the critical coupling at the channel-symmetric point [30]. Therefore, on fine-tuning the Kondo coupling $J_a \to J_a^c$ to the symmetric point, the 3CK physics is obtained with the vanishing temperature scale $T^* \to 0$ and a diverging length scale ξ^* $(\sim 1/T^*) \to \infty$ at the lowest-energy scales. On the other hand, similar to the 2CK model, in the channel-asymmetric case, it is expected that there is no correlation between a decoupled channel and the impurity, namely, the total correlation in a decoupled channel is 0.

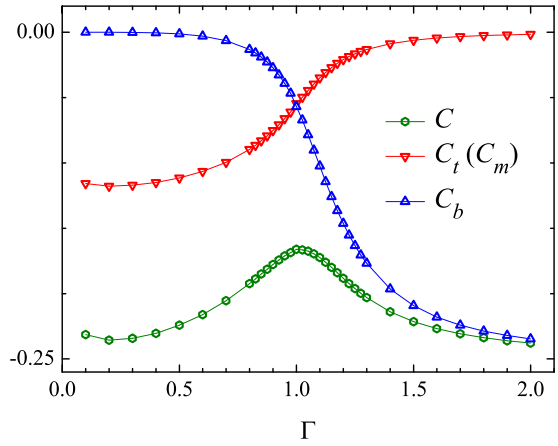

FIG. 5. Ground-state spin correlations C, C_t (C_m), and C_b between the localized impurity and electrons in the electronic channels in the 3CK model versus Γ for a system of size $N = 199$ with fixed coupling $J = 1$.

By using the NORG method, we have also studied the 3CK model (3) illustrated in Fig. 1(b). Figure 5 shows the calculated spin correlation with the fixed coupling $J = 1$. As we see, $C_b \to 0$ when the parameter $\Gamma \ll 1$, indicating that the bottom channel decouples while the impurity is correlated equally with the top and middle channels. In contrast, when the parameter $\Gamma \gg 1$, $C_b \to -\frac{1}{4}$ while C_t (or C_m) $\to 0$, demonstrating that the impurity is correlated only with the bottom channel while the other two channels decouple. At the channel-symmetric point, the impurity is correlated equally with all the channels, as shown by C_t, C_m, and C_b crossing at the critical point $\Gamma = 1$. On the other hand, for a small parameter $\Gamma \ll 1$, where the impurity is overscreened by the top and middle channels, there is an uptick instead of a monotonic decrease towards $-\frac{1}{4}$ for the curves of C_t (C_m) and C. This results from the nonmonotonic dependence of the Kondo temperature T_K on the Kondo coupling $J_0 = J/\Gamma$ for the 2CK model, where T_K depends exponentially on $1/J_0$ and J_0 in the two regimes of small and large coupling, respectively [45].

In comparison with the case of the 2CK model, the definition of the spin-correlation ratio R_C is given by

$$R_C = \frac{C_b}{C} = \frac{\sum_i \langle 0|S_0^z s_{bi}^z|0\rangle}{\sum_{ai} \langle 0|S_0^z s_{ai}^z|0\rangle}. \tag{8}$$

Accordingly, similar to the 2CK model, at the channel-symmetric point $\Gamma = 1$, the overscreened impurity is correlated equally with all the channels, leading to $R_C = \frac{1}{3}$. On the other hand, for any $\Gamma > 1$, the impurity is correlated only with the bottom channel, while the other two channels decouple. In contrast, for any $\Gamma < 1$, the bottom channel decouples and the impurity is correlated equally with the top and middle channels. As a result, the value of R_C is expected to go from 0 to 1 around the critical point $\Gamma = 1$. The calculated spin-correlation ratio R_C and its derivative $R_C' = \partial R_C/\partial\Gamma$ with respect to Γ are presented in Figs. 6(a) and 6(b), respectively. As we see, the value of R_C goes from 0 to 1 around the critical point $\Gamma = 1$ and R_C' peaks at $\Gamma = 1$ with this peak sharpening as the system size N increases, indicating that

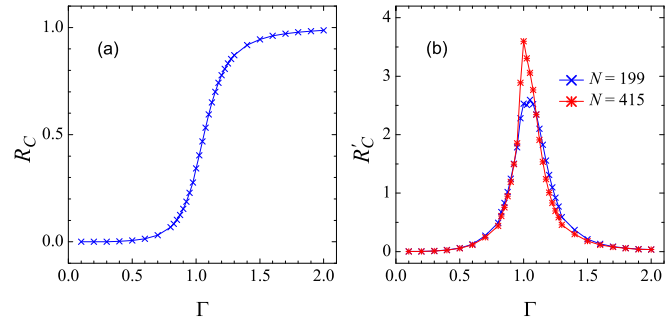

FIG. 6. (a) Spin-correlation ratio R_C as a function of Γ for a system of size $N = 199$ and (b) derivative of R_C with respect to Γ, namely, $R_C' = \partial R_C/\partial\Gamma$, for systems of different size N with fixed coupling $J = 1$ in the 3CK model.

R_C' goes to diverge at the channel-symmetric point $\Gamma = 1$ in the thermodynamic limit. Consequently, the behaviors of R_C and R_C' in the 3CK model are similar to those in the 2CK model.

Likewise, the same finite-size scaling form of Eq. (7) for R_C is used in the 3CK model. Here the correlation length is taken as the critical crossover scale ξ^* at which the RG flow crosses over from the overscreened 3CK fixed point to the fully screened Fermi-liquid fixed point ($\Gamma > 1$) or to the overscreened 2CK fixed point ($\Gamma < 1$). The corresponding results are presented in Figs. 7(a) and 7(b) for fixed Kondo couplings $J = 1.0$ and $J = 0.5$, respectively. We find that the best data collapse is achieved by $\nu = 2.5 \pm 0.1$ and $\beta = 0.10 \pm 0.01$, with $\nu = 2.5$ being in agreement with the result of CFT [12,44]. Moreover, the values of the critical exponent β for both the 2CK and 3CK models are equal to 0.1, which is not given in CFT studies. Thus, the spin-correlation ratio R_C acts as an appropriate order parameter for characterizing the IQPTs in both the 2CK and 3CK models.

IV. DISCUSSION

Impurity quantum phase transitions occur in various quantum impurity systems at zero temperature. The multichannel Kondo system, associated with the intermediate-coupling fixed point showing non-Fermi-liquid behavior, is a paradigm

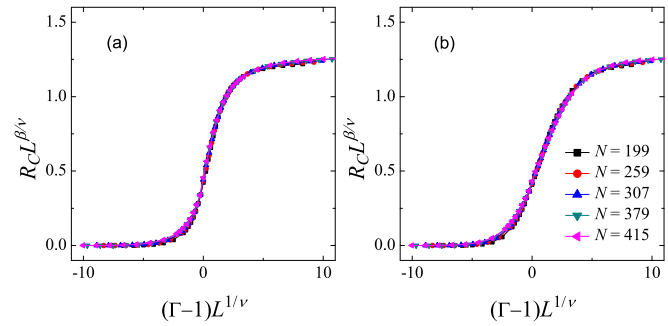

FIG. 7. Finite-size scaling of the spin-correlation ratio R_C with Kondo couplings (a) $J = 1.0$ and (b) $J = 0.5$ in the 3CK model, respectively. The values obtained are $\beta = 0.10 \pm 0.01$ and $\nu = 2.5 \pm 0.1$.

for exploring IQPTs. According to the CFT, the nontrivial low-temperature properties of an MCK system are determined by the leading irrelevant operator at the overscreened fixed point [12]. Specifically, for an MCK model which obeys $SU(2)_{spin} \times SU(M)_{channel}$ symmetry, it has been proved that the dimension of the leading irrelevant operator is $1 + \Delta = 1 + 2/(2 + M)$; for example, the impurity magnetic susceptibility $\chi_{imp} \propto T^{2\Delta-1}$ when $T \to 0$ except $M = 2$. On the other hand, at zero temperature, an IQPT can be driven by the channel asymmetry, i.e., the $SU(M)_{channel}$ symmetry is broken. More specifically, when one of the couplings is increased, the ground state of the system will transit into a Fermi-liquid phase. In contrast, when one of the couplings is decreased, the ground state will behave as that of an $(M - 1)$-channel Kondo model with a non-Fermi-liquid phase ($M > 2$). For this critical transition, the critical exponent ν of the correlation length is $1/\Delta$, with Δ the dimension of the most relevant new operator that appears in the Hamiltonian when the channel symmetry is broken [14,46]. Thus, for the 2CK model $\nu = 2$ and for the 3CK model $\nu = 2.5$. As shown in this work, these generic properties are well manifested by the spin-correlation calculations for the 2CK and 3CK models. In particular, the calculated critical exponents ν are the same as those given by the CFT. Furthermore, the calculations give extra information beyond the CFT, namely, the critical exponent β of the order parameter.

V. SUMMARY

We have introduced an order parameter, namely, spin-correlation ratio R_C, for describing IQPTs in the multichannel Kondo system driven by channel asymmetry, based on spin correlation between the impurity and electrons in the electronic channels. By the calculations using the NORG method, we demonstrated that the spin-correlation ratio R_C is an appropriate order parameter for describing the IQPTs. By finite-size-scaling analysis, the critical exponents β of R_C and ν of the correlation length are further determined to be $\beta = 0.10(1)$ and $\nu = 2.0(1)$ for the 2CK model and $\beta = 0.10(1)$ and $\nu = 2.5(1)$ for the 3CK model. Moreover, the values of the critical exponent $\nu = 1/\Delta$ are the same as the results of the conformal field theory for the multichannel Kondo system.

ACKNOWLEDGMENTS

This work was supported by National Natural Science Foundation of China (Grants No. 11934020 and No. 11874421). R.-Q.H. was supported by the Fundamental Research Funds for the Central Universities and the Research Funds of Renmin University of China (Grant No. 18XNLG11). Computational resources were provided by National Supercomputer Center in Guangzhou with the Tianhe-2 Supercomputer and Physical Laboratory of High Performance Computing at RUC.

[1] J. Kondo, Prog. Theor. Phys. **32**, 37 (1964).
[2] A. Hewson, *The Kondo Problem to Heavy Fermions* (Cambridge University Press, Cambridge, 1997).
[3] K. G. Wilson, Rev. Mod. Phys. **47**, 773 (1975).
[4] R. Bulla, T. A. Costi, and T. Pruschke, Rev. Mod. Phys. **80**, 395 (2008).
[5] P. Nozières and A. Blandin, J. Phys. (Paris) **41**, 193 (1980).
[6] N. Andrei and C. Destri, Phys. Rev. Lett. **52**, 364 (1984).
[7] A. M. Tsvelick and P. B. Wiegmann, Z. Phys. B **54**, 201 (1984).
[8] A. M. Tsvelick, J. Phys. C **18**, 159 (1985).
[9] N. Andrei and A. Jerez, Phys. Rev. Lett. **74**, 4507 (1995).
[10] G. Zaránd, T. Costi, A. Jerez, and N. Andrei, Phys. Rev. B **65**, 134416 (2002).
[11] I. Affleck and A. W. W. Ludwig, Phys. Rev. Lett. **67**, 161 (1991).
[12] I. Affleck and A. W. W. Ludwig, Nucl. Phys. B **360**, 641 (1991).
[13] I. Affleck, A. W. W. Ludwig, H. B. Pang, and D. L. Cox, Phys. Rev. B **45**, 7918 (1992).
[14] I. Affleck and A. W. W. Ludwig, Phys. Rev. B **48**, 7297 (1993).
[15] O. Parcollet, A. Georges, G. Kotliar, and A. Sengupta, Phys. Rev. B **58**, 3794 (1998).
[16] V. J. Emery and S. Kivelson, Phys. Rev. B **46**, 10812 (1992).
[17] D. G. Clarke, T. Giamarchi, and B. I. Shraiman, Phys. Rev. B **48**, 7070 (1993).
[18] H. B. Pang and D. L. Cox, Phys. Rev. B **44**, 9454 (1991).
[19] A. M. Sengupta and A. Georges, Phys. Rev. B **49**, 10020 (1994).
[20] M. Fabrizio, A. O. Gogolin, and P. Nozières, Phys. Rev. Lett. **74**, 4503 (1995).
[21] T. Cichorek, A. Sanchez, P. Gegenwart, F. Weickert, A. Wojakowski, Z. Henkie, G. Auffermann, S. Paschen, R. Kniep, and F. Steglich, Phys. Rev. Lett. **94**, 236603 (2005).
[22] R. M. Potok, I. G. Rau, S. Hadas, O. Yuval, and D. Goldhaber-Gordon, Nature (London) **446**, 167 (2007).
[23] H. T. Mebrahtu, I. V. Borzenets, H. Zheng, Y. V. Bomze, A. I. Smirnov, S. Florens, H. U. Baranger, and G. Finkelstein, Nat. Phys. **9**, 732 (2013).
[24] A. J. Keller, L. Peeters, C. P. Moca, I. Weymann, V. Mahalu, D. Umansky, D. Zaránd, and D. Goldhaber-Gordon, Nature (London) **526**, 237 (2015).
[25] Z. Iftikhar, S. Jezouin, A. Anthore, U. Gennser, and F. Pierre, Nature (London) **526**, 233 (2015).
[26] L. J. Zhu, S. H. Nie, P. Xiong, P. Schlottmann, and J. H. Zhao, Nat. Commun. **7**, 10817 (2015).
[27] T. Cichorek, L. Bochenek, M. Schmidt, A. Czulucki, G. Auffermann, R. Kniep, R. Niewa, F. Steglich, and S. Kirchner, Phys. Rev. Lett. **117**, 106601 (2016).
[28] A. K. Mitchell, M. Becker, and R. Bulla, Phys. Rev. B **84**, 115120 (2011).
[29] M. Vojta, Philos. Mag. **86**, 1807 (2006).
[30] A. K. Mitchell, M. R. Galpin, S. Wilson-Fletcher, D. E. Logan, and R. Bulla, Phys. Rev. B **89**, 121105(R) (2014).
[31] A. Bayat, H. Johannesson, S. Bose, and P. Sodano, Nat. Commun. **5**, 3784 (2014).
[32] B. Alkurtass, A. Bayat, I. Affleck, S. Bose, H. Johannesson, P. Sodano, E. S. Sørensen, and K. Le Hur, Phys. Rev. B **93**, 081106(R) (2016).
[33] A. Bayat, Phys. Rev. Lett. **118**, 036102 (2017).
[34] R.-Q. He and Z.-Y. Lu, Phys. Rev. B **89**, 085108 (2014).

[35] Y. Wang, E. Walter, S. S. B. Lee, K. M. Stadler, J. von Delft, A. Weichselbaum, and G. Kotliar, Phys. Rev. Lett. **124**, 136406 (2020).
[36] R.-Q. He, J. Dai, and Z.-Y. Lu, Phys. Rev. B **91**, 155140 (2015).
[37] R. Zheng, R.-Q. He, and Z.-Y. Lu, Chin. Phys. Lett. **35**, 067301 (2018).
[38] C. Lin and A. A. Demkov, Phys. Rev. B **88**, 035123 (2013).
[39] M. N. Barber, in *Phase Transitions and Critical Phenomena*, edited by C. Domb and J. L. Lebowitz (Academic, London, 1983), Vol. 8, pp. 145–477.
[40] K. S. D. Beach, L. Wang, and A. W. Sandvik, arXiv:cond-mat/0505194.
[41] M. Campostrini, A. Pelissetto, and E. Vicari, Phys. Rev. B **89**, 094516 (2014).
[42] Y. Otsuka, S. Yunoki, and S. Sorella, Phys. Rev. X **6**, 011029 (2016).
[43] S. Sachdev, *Quantum Phase Transitions* (Cambridge University Press, New York, 2011).
[44] I. Affleck, A. W. W. Ludwig, and B. A. Jones, Phys. Rev. B **52**, 9528 (1995).
[45] C. Kolf and J. Kroha, Phys. Rev. B **75**, 045129 (2007).
[46] I. Affleck, J. Phys. Soc. Jpn. **74**, 59 (2005).